Six-site polarizable model of water based on the classical Drude oscillator

Wenbo Yu, Pedro E. M. Lopes, Benoît Roux, and Alexander D. MacKerell Jr.

Citation: The Journal of Chemical Physics **138**, 034508 (2013); doi: 10.1063/1.4774577
View online: http://dx.doi.org/10.1063/1.4774577
View Table of Contents: http://scitation.aip.org/content/aip/journal/jcp/138/3?ver=pdfcov
Published by the AIP Publishing

Articles you may be interested in

United polarizable multipole water model for molecular mechanics simulation
J. Chem. Phys. **143**, 014504 (2015); 10.1063/1.4923338

Size effects on water adsorbed on hydrophobic probes at the nanometric scale
J. Chem. Phys. **138**, 214702 (2013); 10.1063/1.4807092

Intermolecular shielding contributions studied by modeling the C 13 chemical-shift tensors of organic single crystals with plane waves
J. Chem. Phys. **131**, 144503 (2009); 10.1063/1.3225270

A simple polarizable model of water based on classical Drude oscillators
J. Chem. Phys. **119**, 5185 (2003); 10.1063/1.1598191

Solvent effect on the nuclear magnetic shielding: ab initio study by the combined reference interaction site model and electronic structure theories
J. Chem. Phys. **115**, 8949 (2001); 10.1063/1.1412872

Reuse of AIP Publishing content is subject to the terms: https://publishing.aip.org/authors/rights-and-permissions. Downloaded to IP: 129.15.64.216 On: Sun, 25 Sep 2016 17:34:16

Six-site polarizable model of water based on the classical Drude oscillator

Wenbo Yu,[1] Pedro E. M. Lopes,[1] Benoît Roux,[2] and Alexander D. MacKerell, Jr.[1,a)]
[1]*Department of Pharmaceutical Sciences, School of Pharmacy, University of Maryland, 20 Penn Street, Baltimore, Maryland 21201, USA*
[2]*Department of Biochemistry and Molecular Biology, University of Chicago, Chicago, Illinois 60637, USA*

(Received 6 August 2012; accepted 21 December 2012; published online 18 January 2013)

A polarizable water model, SWM6, was developed and optimized for liquid phase simulations under ambient conditions. Building upon the previously developed SWM4-NDP model, additional sites representing oxygen lone-pairs were introduced. The geometry of the sites is assumed to be rigid. Considering the large number of adjustable parameters, simulated annealing together with polynomial fitting was used to facilitate model optimization. The new water model was shown to yield the correct self-diffusion coefficient after taking the system size effect into account, and the dimer geometry is better reproduced than in the SWM4 models. Moreover, the experimental oxygen-oxygen radial distribution is better reproduced, indicating that the new model more accurately describes the local hydrogen bonding structure of bulk phase water. This was further validated by its ability to reproduce the experimental nuclear magnetic shielding and related chemical shift of the water hydrogen in the bulk phase, a property sensitive to the local hydrogen bonding structure. In addition, comparison of the liquid properties of the SWM6 model is made with those of a number of widely used additive and polarizable models. Overall, improved balance between the description of monomer, dimer, clustered, and bulk phase water is obtained with the new model compared to its SWM4-NDP polarizable predecessor, though application of the model requires an approximately twofold increase on computational resources. © *2013 American Institute of Physics*. [http://dx.doi.org/10.1063/1.4774577]

I. INTRODUCTION

Computational approaches based on empirical force fields are widely used as routine techniques to study biomolecules, facilitating the interpretation of experimental results as well as allowing for predictions that motivate experimental studies.[1] As the most common solution for biological processes, a water model is always the starting point for any force field development effort toward a full description of biomolecular systems.[2] Biomolecular force fields are based on simple parametric energy functions, and the quality of the force field parameters determines the reliability of the computational results. An ideal force field model of water should correctly reproduce the structural, thermodynamic, and dynamic behavior of water. However, due to its unique set of physical and chemical properties, development of a water model based on a simple energy function that accurately reproduces a wide range of water properties is still a challenging task and being revisited continuously.[3–5]

Many classical force field models, in which the energy function treats the nonbond terms in a pairwise additive fashion and implicitly incorporates induced polarization by optimizing the fixed partial atomic charges to yield average polarizable induction in the bulk phase, have been developed for water.[6–14] While commonly employed in simulations, such as the TIP3P model,[8] additive models have the inability to capture the sensitive polarizable feature of water, and thus result in unbalanced descriptions among its microscopic and bulk properties. For example, additive water models usually overestimate the zero-field dipole moment in order to get better performance on bulk properties.[9] To overcome this limitation, polarizable water models that explicitly treat the polarization via different techniques including induced dipoles, fluctuating charges, and the classical Drude oscillator (or Shell model), have been developed in recent years.[15–22]

With explicit polarization implemented using the classical Drude oscillator model,[23–25] the SWM4-DP (SWM represents "simple water model" and DP represents "Drude polarization") and the subsequent SWM4-NDP model (NDP represents "negative Drude polarization") of water were introduced into the CHARMM family of force fields.[26,27] Targeting four important bulk properties, vaporization enthalpy, density, static dielectric constant, and self-diffusion coefficient, the optimized models were shown to have better performances than additive models and outperform many of the polarizable models available at that time. Specifically, the models have a good balance between the treatment of single, clustered, and bulk phase water, and perform well in simulations under ambient conditions.[28–30] However, some drawbacks are also present that motivated the present effort. First, in the development of the SWM4 models, the diffusion coefficient, which was used as target data, was evaluated without system size correction. It has been shown that, unlike other dynamical properties such as viscosity, diffusion coefficients calculated using molecular dynamics (MD) with periodical boundary condition (PBC) are system size dependent and simulations on a small number of water

a)Author to whom correspondence should be addressed. Electronic mail: alex@outerbanks.umaryland.edu.

 © 2013 American Institute of Physics

Reuse of AIP Publishing content is subject to the terms: https://publishing.aip.org/authors/rights-and-permissions. Downloaded to IP: 129.15.64.216 On: Sun, 25 Sep 2016 17:34:16

molecules will result in underestimation of the diffusion coefficient.[31] Thus, with the optimized model targeting the uncorrected data, the actual value for the diffusion coefficient of SWM4-DP and SWM4-NDP is expected to be overestimated (see below). Second, as pointed out in the development of SWM4-DP model,[26] the water dimer displayed an acceptor angle of 70° as compared to the experimental value[32] of 58°, resulting in an underestimated total dipole moment of the dimer. This was the results of empirical optimization aimed at reproducing the tetrahedral hydrogen bonding pattern in bulk water, a property that represents a challenge for a rigid four-site model. Thus, with such a compromise, the hydrogen bonding structures cannot be reproduced perfectly for both microscopic (i.e., dimers and clusters) and bulk water. Finally, during development of the biomolecular Drude force field, lone pairs (LP) were introduced on hydrogen bond acceptors;[33] however, LPs are not present on the SWM4 models, which may be considered a limitation that may also contribute to less than ideal treatment of hydrogen bonding.

The goal of present paper is to develop a new model of water based on the existing SWM4-NDP model that overcomes the two main issues discussed above while maintaining the performance of the remaining properties. This largely involves optimization of a new model that will yield improved balance between the description of microscopic and bulk phase water based on improved hydrogen bonding geometries. It should be noted that several new polarizable models of water were published after the SWM4 series of models and designed for different purposes.[34–37] For example, TTM3-F model was designed to accurately describe the energies of small water clusters and vibrational spectra of water.[34] As most biomolecular simulations are done under ambient conditions, the current new model of water is designed to target properties of water under room temperature and pressure conditions.

II. THEORY AND METHODS

A. Functional form of the model

To make the new model simple and consistent with the existing SWM4-NDP model, only rigid models with fixed geometry and fixed charge sites were considered. The inclusion of LPs in the model is expected to improve the geometry of the water dimer. A good illustration is the TIP5P water model, that, with the help of LP sites, yields a tetrahedral orientation and results in an acceptor angle that is closer to the experimental value when compared to the TIP4P water model.[9] However, a five-site rigid model with a reasonable LP geometry significantly underestimates the quadrupole moment of the water monomer,[9] which was shown to lead to an incorrect dielectric constant of bulk phase water.[38] For example, the Q_{xx}, Q_{yy}, and Q_{zz} components of the TIP5P model are −0.17, 1.65, and −1.48 DÅ, respectively,[9] as compared to experimental values of −0.13, 2.63, and −2.50 DÅ. To further illustrate this, Figure 1 presents the dependence of the quadrupole moments on the LP geometry for a five-site water model with no charge on the oxygen and when the dipole moment is fixed to the experimental value of 1.85 D.[39] If one wants to get a reasonable quadrupole moment, an unphysical LP geometry is needed. For example, to get quadrupole moments similar to a four-site model, the distance between the oxygen atom and LPs (r_{OL}) need to be as large as 1.8 Å when the LP intervening angle θ_{LOL} is a physically reasonable value of 110° as shown in Figure 1. Similar results are obtained if the partial atomic charges are also distributed on the oxygen atom in a rigid five-site water model (Figure S1 of the supplementary material[40]). While, in principle, such a model would be possible, the position of the LPs would be close to the van der Waals surface of their parent oxygen as judged by the Lennard-Jones (L-J) R_{min} parameter, leading to instabilities in molecular mechanics (MM) calculations.

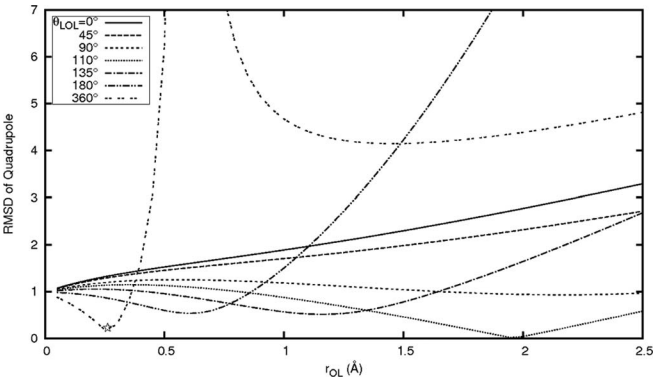

FIG. 1. Dependence of the calculated quadrupole moments on the LP geometries for a five-site water model with zero charge on the oxygen. The permanent dipole is fixed to be 1.85 D. RMSD of the quadrupole is given by $\sqrt{\frac{[Q_{xx}(cal)-Q_{xx}(\exp)]^2+[Q_{yy}(cal)-Q_{yy}(\exp)]^2+[Q_{zz}(cal)-Q_{zz}(\exp)]^2}{3}}$. When the $\theta_{LOL} = 360°$, the five-site model is equivalent to a four-site model and the star indicates the value of the SWM4-NDP model.

Indeed, the importance of reproducing the quadrupole moments as well as the dipole moment by a water model is well known[14,41] and many water models explicitly incorporate quadrupole moments such as the SSDQO[42] and AMOEBA[15] water models. Though many liquid properties such as density and heat of vaporization are only sensitive to the dipole moment, quadrupole moments were shown to be more important in many other aspects.[43–45] And since the SWM4-NDP model already describes the quadrupole moments very well by utilizing an auxiliary site (M site), it was decided that a five-site model was not an appropriate model to improve upon the SWM4-NDP model. Thus a six-site model, for which LP sites were introduced as small perturbations to the existing four-site model, was pursued. It was anticipated that such a model may yield an improved description of the water dimer geometry without losing the description of quadrupole moments which will benefit from the M site as defined in a four-site rigid model. Interestingly, Niu *et al.* reported that six partial charge sites are necessary to account for the large quadrupole of water.[46] This was attributed to the *p*-orbital character perpendicular to the water plane as well as a shift of negative charge toward the hydrogens; these three regions correspond well with the locations of the LP and M sites, respectively, in the current model.

The functional form of the current model may, therefore, be considered a hybrid of the TIP5P and SWM4-NDP models and the geometry of the model is depicted in Figure 2. The water molecule is kept in its experimental gas

Reuse of AIP Publishing content is subject to the terms: https://publishing.aip.org/authors/rights-and-permissions. Downloaded to IP: 129.15.64.216 On: Sun, 25 Sep 2016 17:34:16

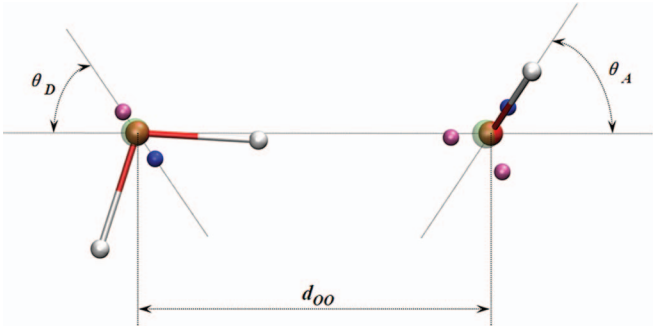

FIG. 2. Geometry of the SWM6 water dimer. The water model is represented by an oxygen atom (red), a Drude oscillator linked to the oxygen (green), two hydrogen atoms (white), M site (blue), and two LP sites (pink). The dimer geometry parameters, the oxygen-oxygen distance, d_{OO}, the donor angle, θ_D, and the acceptor angle, θ_A, are shown.

phase geometry[47] with an O-H bond length r_{OH} of 0.9572 Å and a H–O–H valence angle θ_{HOH} of 104.52°. Six interaction sites are defined including one oxygen and two hydrogen atoms, one massless site (M site) located at a fixed distance r_{OM} from the oxygen atom along the bisector of the H–O–H angle, and two additional massless sites (LP sites) located at a fixed distance r_{OL} from the oxygen atom in the plane perpendicular to the water plane and separated by an intervening angle θ_{LOL}. The explicit polarization is introduced by a classical Drude oscillator attached to the oxygen atom through a harmonic spring with force constant k_D. Unlike the SWM4-NDP and TIP5P models, where the oxygen atom carries no charge in the zero field, a positive charge $q_O{}^0$ was put on the oxygen atom in the new model as preliminary tests showed that, without this additional degree of freedom in the parameter space, no optimal models could be found to reasonably reproduce both the gas phase and bulk phase properties. As the oxygen atom carries the Drude polarizability of the model, it does carry charge in a non-zero field even if its partial charge was zero, thus such additional zero field charge on the oxygen does not increase the computational costs of the model. The permanent molecular dipole of the new model is created by positive charges on the hydrogen (q_H) and oxygen ($q_O{}^0$) atoms, and negative charges on LP (q_L) and M (q_M) sites. The induced dipole of the water molecule in a field E created by its surrounding molecules is given by αE, where α is the molecular polarizability and equals $q_D{}^2/k_D$, where q_D is the charge carried by the Drude particle. In this work the Drude was assigned a negative charge, as in the SWM4-NDP model, to represent the electronic degrees of freedom of the molecule. Thus, in a non-zero field, the oxygen atom in the model carries a positive charge q_O that is equal to $q_O{}^0$-q_D and the L-J potential only operates between oxygen atoms with a well depth ε_O and a minimum energy distance $R_{min,O}$. The total potential energy between two water molecules, A and B, is then given by Eq. (1) using the CHARMM Drude polarizable force field functional form,[48]

$$U_{AB}(\{r\}) = \sum_{i=A}^{B} \tfrac{1}{2} k_D (r_{D,i} - r_{O,i})^2 + \sum_{s,s'} \frac{q_s q_{s'}}{|r_{s,A} - r_{s',B}|} + \varepsilon_O \left[\left(\frac{R_{\min,O}}{|r_{O,A} - r_{O,B}|} \right)^{12} - 2 \left(\frac{R_{\min,O}}{|r_{O,A} - r_{O,B}|} \right)^{6} \right], \quad (1)$$

where the Coulombic potentials are calculated between all intermolecular pairs of charged sites s, i.e., oxygen and hydrogen atoms, M and LP sites, and the Drude particle. To maintain consistency with the SWM4-NDP model, the new model with six interaction sites is named SWM6-NDP, or in short, SWM6. It should be noted that there is already an additive six-site water model available, which was designed for simulation of ice and water near the melting point, rather than for liquid water under ambient conditions.[49]

B. Parametrization strategy

Several parameters in the SWM6 model need to be adjusted to obtain an optimal model. Similar to the SWM4-NDP model, a spring constant of 1000 kcal/mol/Å^2 is used for the Drude particle and the associated Drude charge q_D (i.e., the polarizability α) is a free parameter. Also, the permanent dipole of the model is fixed to match the experimental gas phase value of 1.85 D.[39] Thus, for a given geometry to maintain a total charge of zero, only three out of the five charge parameters need to be adjusted. Here we choose $q_O{}^0$, q_L, and α (corresponds to q_D), and together with the three geometric parameters (r_{OM}, r_{OL}, θ_{LOL}) and two L-J parameters (ε_O, $R_{min,O}$), yielding a total of eight parameters that were optimized. Unlike the SWM4-NDP model which was optimized targeting four essential properties of bulk phase water, the SWM6 model was optimized to be able to get the correct dimer geometry in addition to the bulk properties, i.e., targeted properties include quadrupole moments of the monomer, dipole moment, equilibrium acceptor, and donor angles, and potential energy surface (PES) of the dimer, vaporization enthalpy, density, static dielectric constant and self-diffusion coefficient of liquid phase water at ambient conditions. A systematic grid based search in the full parameter space, as used for SWM4-NDP, is not practical considering the additional parameters and target data used for SWM6. To perform the parametrization within a computationally feasible context, a strategy, as will be described below, was designed and a flow chart of the approach can be found in Figure S2 in the supplementary material.[40]

During development of SWM4 models, it was observed that there is a one-to-one correspondence between interaction energy of the water dimer (U_{dimer}) and interaction energy of bulk phase water (Δu) for a small region in parameter space.[26,27] A relationship was also found between the oxygen-oxygen equilibrium distance of the water dimer (d_{OO}) and the molecular volume of bulk phase water ($\langle v \rangle$). Such correspondence between (U_{dimer}, d_{OO}) and (Δu, $\langle v \rangle$) pairs can be used to expedite the parametrization procedure. First, all parameters were adjusted freely, though limited to physically reasonable ranges to yield specific (U_{dimer}, d_{OO}) pairs while targeting experimental data including quadrupole moments of the monomer, dipole moment of the dimer, and equilibrium acceptor, and donor angles of the dimer as well as quantum mechanical (QM) energies from a PES scan of the acceptor angle as defined in Figure 2. This step is designed to locate models yielding specific U_{dimer} and d_{OO} values while

Reuse of AIP Publishing content is subject to the terms: https://publishing.aip.org/authors/rights-and-permissions. Downloaded to IP: 129.15.64.216 On: Sun, 25 Sep 2016 17:34:16

reproducing other monomer and dimer properties. Several models were optimized to yield combinations of the following values: $U_{dimer} = -5.30, -5.15, -5.00, -4.85$ kcal/mol, and $d_{OO} = 2.77, 2.79, 2.81, 2.83$ Å. Simulated annealing (SA) optimization[50,51] was employed using the algorithm of Goffe *et al.*[52] to facilitate this step. Starting with a temperature of 500 K, the SA method minimized a predefined error function by successively adjusting parameters at each step and either accepting or rejecting the new parameter set based on the Metropolis criterion.[51] The temperature was gradually reduced to near 0 K at the end of a SA run to obtain converged result. The error function is the sum of all differences between MM and experimental or QM data for all properties mentioned above with appropriate weighting factors. The weighting factors were determined from several test runs to achieve a balanced contribution of the different terms to the error function. The weighting factors for differences on U_{dimer} and d_{OO} were set to be relatively large to ensure the obtained parameter set yields the targeted values of these two properties. Details about the SA setup and the error function can be found in the supplementary material.[40]

The models generated from the first step were then used to calculate Δu and $\langle v \rangle$ from short time MD simulations. This step was iterated with the first step until a model was identified that yields values of both Δu and $\langle v \rangle$ close to the corresponding experimental data. Then based on this model, a $3 \times 3 \times 3 \times 3 \times 3 \times 3 \times 3 \times 3$ grid spanning local parameter space was used to generate 6560 models (i.e., 3 values as $x\text{-}\delta_x$, x, and $x+\delta_x$ for each parameter around the current optimal value x with a small parameter grid size δ_x, results in 6561 combinations including the original model) and short time MD simulations were performed to calculate Δu, $\langle v \rangle$, average dipole $\langle \mu \rangle$ and height of the first peak in the oxygen-oxygen radial distribution function $g_{OO}^{(1)}$. The last two properties were used to help to indirectly target the dielectric constant ε and uncorrected diffusion coefficient D_{PBC} which cannot be accurately evaluated from short time MD simulations but have strong correlations with $\langle \mu \rangle$ and $g_{OO}^{(1)}$ as observed during development of the SWM4 models. Several long time MD simulations were performed to explore the correlations between $(\langle \mu \rangle, g_{OO}^{(1)})$ and (ε, D_{PBC}), showing that in order to obtain the experimental value for ε, $\langle \mu \rangle$ should be approximately 2.43 D, and a value close to 3.10 for $g_{OO}^{(1)}$ is needed for a correct D_{PBC} value. Here the target value of D_{PBC} was evaluated using the method of Yeh and Hummer[31] with the experimental data[53,54] of diffusion coefficient D_0 and viscosity η. From the MD simulations, four second-order polynomial interpolation formulas P (α, q_O^0, q_L, r_{OM}, r_{OL}, θ_{LOL}, ε_O, $R_{min,O}$) were fitted for the four properties using the R program,[55] and the optimal model was selected as the starting point for next round of optimization. Then another $3 \times 3 \times 3 \times 3 \times 3 \times 3 \times 3 \times 3$ grid with reduced parameter ranges around the optimal model was used to generate an additional 6560 models and the four properties for each model were evaluated from the fitted polynomial formulas. The top models given by the polynomial formulas were then subjected to short-time MD simulations to validate the predictions. If large differences between the predicted and MD results were found, then these MD results were added to the previous MD results and used for new polynomial fitting. Such polynomial fitting and MD validation were repeated until a model that reproduces the target data to a high level of accuracy was located.

C. Computational details

All empirical force field calculations were performed using version 36 of CHARMM.[48] Gas phase MM energy minimizations of the water dimer were performed using the adopted basis Newton-Raphson (ABNR) minimization algorithm to a gradient tolerance of 10^{-5} kcal/(mol Å) with an infinite nonbonded cutoff distance. MM PES scans of the water dimer were performed by building the rigid geometries in CHARMM and harmonic restraints with force constant of 10 000 kcal/(mol rad) were placed on the scanned degrees of freedom followed by minimization of all other degrees of freedom. The bulk phase properties of the SWM6 models were calculated using MD simulations performed on 216 water molecules in a cubic box with PBCs. The particle mesh Ewald summation method[56] with a coupling parameter of 0.33 for the charge screening and fourth-order spline for the mesh interpolation was used to treat electrostatic interactions. The nonbond pair lists were maintained out to 18 Å and a real space cutoff of 15 Å was used for both electrostatic and L-J interactions with a isotropic long-range correction used for the L-J term.[57] MD simulations were performed in the isothermal-isobaric (NPT) ensemble using the velocity Verlet (VV2) integrator[58] and extended Lagrangian double-thermostat formalism with the TPCONTROL module implemented in CHARMM.[25] A Nosé-Hoover thermostat[59,60] was applied to all non-Drude atoms to control the global temperature of 298.15 K for the whole system. A second Nosé-Hoover thermostat was used to control the relative motion of each oxygen-Drude pair at a low temperature of 1 K to ensure that the time course of induced dipoles stays close to the self-consistent field regimen. A modified Anderson-Hoover barostat was used to maintain the system at constant pressure of 1 atm. A relaxation time of 5 fs was used for the Drude oscillator thermostat while 0.1 ps was used for the main thermostat and the barostat. The water molecules were kept rigid during the simulation by SHAKE/Roll and RATTLE/Roll procedures.[58] During the optimization, each model was simulated for 150 ps with the first 50 ps treated as equilibration and a time step of 1 fs was used.

For the final optimal SWM6 model, various microscopic and bulk phase properties were evaluated. For comparison purpose, properties were also calculated with the same simulation setups for the SWM4-NDP model. Properties of the water dimer were calculated in the same way as described above in the model optimization stage. QM PESs of the dimer were performed at the MP2/aug-cc-pVTZ level[61,62] with tight tolerances using the GAUSSIAN 03 program.[63] To characterize the binding energies of gaseous water clusters, QM geometries were read into CHARMM, the individual water intramolecular geometries set to the MM values and the cluster subjected to an ABNR minimization to a gradient

Reuse of AIP Publishing content is subject to the terms: https://publishing.aip.org/authors/rights-and-permissions. Downloaded to IP: 129.15.64.216 On: Sun, 25 Sep 2016 17:34:16

tolerance of 10^{-5} kcal/(mol Å). To calculate liquid properties, 40 independent MD simulations in the NPT ensemble starting from the same initial coordinates but with different random initial velocities were performed for 150 ps. Averaged properties and uncertainties were then calculated from the last 100 ps of each simulation and result in a total of 4 ns of MD sampling. To investigate the impact of system size and simulation time on the calculated properties, five additional independent 4 ns MD simulations were performed for a water box of 1000 molecules. For dynamic properties such as viscosity and relaxation times, 40 independent MD simulations in the microcanonical ensemble (NVE) were performed for 150 ps each to avoid artificial perturbations from the extended Lagrangian degrees of freedom. The initial coordinates for the NVE MD simulations were collected from 40 state points from a MD trajectory in the canonical ensemble (NVT) at 298.15 K and a constant volume corresponding to the average density calculated from the above described NPT simulations. The last 100 ps of simulation time from each NVE simulation was used for analyses. To calculate the air/water interface properties, a system of 216 waters contained in an L × L × L cube was simulated in slab geometry in an L × L × 3L rectangular PBC cell. With this PBC setup, two separated vacuum/water interfaces were maintained during the MD simulation. Here L corresponds to the average density of the model that is 18.65Å for SWM6 model and 18.66 Å for SWM4-NDP model. Five independent MD simulations in the NVT ensemble were equilibrated for 100 ps followed by a 1 ns production run resulting in a total sampling time of 5 ns.

The free energy of hydration was obtained using the free energy perturbation method and calculated as a sum of dispersion, repulsion, and electrostatic contributions, which were calculated with the linear coupling scheme.[64] The weighted histogram analysis method[65] was used to obtain free energies from 300 ps production MD simulations and contributions with different staging parameters were summed. The final value was averaged from ten such calculations from independent MD simulations initiated with different initial velocities.

To further examine the ability of the new water model to reproduce the local hydrogen bonding structure in the bulk phase, nuclear magnetic shielding of the water hydrogen atoms, which is a sensitive indicator of the hydrogen bonding, was calculated. The approach developed by Sebastiani and Parrinello,[66] which was shown to give good estimation of NMR shifts,[67] was used. Similar to the procedures adopted by Banyai *et al.*,[68] 30 structures were extracted from a NPT MD trajectory of a system of 32 water molecules and the nuclear magnetic shieldings were calculated with the BLYP method[69,70] and the Goedecker type pseudopotentials[71] for the two hydrogen atoms in all water molecules, using the NMR module implemented in the CPMD program.[72] This results in $2 \times 32 \times 30 = 1920$ data points for which the average was evaluated to represent the final nuclear magnetic shielding of the water hydrogens for the SWM6 model. For comparison, this property was also calculated for TIP4P-Ew,[12] TIP4P/2005,[13] TIP5P-Ew,[14] SWM4-NDP and a modified version of TIP3P model[73] included in the CHARMM additive force field.

TABLE I. Parameters defining the TIP3P, SWM4-NDP, and SWM6 water models.

	TIP3P[a]	SWM4-NDP[b]	SWM6
Geometric			
r_{OH} (Å)	0.9572	0.9572	0.9572
θ_{HOH} (°)	104.52	104.52	104.52
r_{OM} (Å)		0.24034	0.247
r_{OL} (Å)			0.315
θ_{LOL} (°)			101.098
Electrostatic			
q_O (e)	−0.834	1.71636	1.91589
q_H (e)	0.417	0.55733	0.53070
q_M (e)		−1.11466	−1.13340
q_L (e)			−0.10800
q_D (e)		−1.71636	−1.62789
k_D (kcal/mol/Å^2)		1000	1000
L-J			
ε_O (kcal/mol)	0.1521	0.21094	0.162
$R_{min,O}$ (Å)	3.5364	3.57386	3.590

[a]Reference 9.
[b]Reference 27.

III. RESULTS AND DISCUSSION

A. Optimal model

The parameters defining the optimal SWM6 model are presented in Table I along with parameters of the SWM4-NDP and the original additive TIP3P model. Compared to other sites in the SWM6 model, the LP sites carry a relatively small negative charge. This is consistent with the designed purpose that the LPs are introduced as small perturbations to the four-site model to improve the hydrogen bonding structure of water while maintaining the reproduction of the other properties. Nonetheless, distinct differences of the parameters are found between the SWM6 and SWM4-NDP models. The L-J parameter ε_O of the SWM6 model is smaller than that of SWM4-NDP though $R_{min,O}$ is similar. This suggests that the SWM6 electrostatic terms make a larger contribution to the bulk properties relative to the van de Waals portion of the nonbond interactions. Compared with the two polarizable models, the TIP3P model has a smaller L-J parameter $R_{min,O}$ which is consistent with its smaller equilibrium oxygen-oxygen distance of the water dimer and smaller molecular volume of bulk phase water as listed in Table II. The SWM6 model has a smaller polarizability as compared to the SWM4-NDP model. As presented in Table II, the molecular polarizability of the SWM6 water model is 10% smaller than that of the SWM4-NDP model, resulting in a scaling factor of 0.61 compared to 0.68 for SWM4-NDP. This may be attributed to the additional charge sites in the SWM6 model that partially describe the dipole and higher order moments in the bulk phase and allow the use of a smaller explicit polarization.

B. Monomer and dimer

Similar to the two SWM4 models, the permanent dipole of the isolated water molecule is set to the experimental value of 1.85 D for the SWM6 model. With a negative charge

Reuse of AIP Publishing content is subject to the terms: https://publishing.aip.org/authors/rights-and-permissions. Downloaded to IP: 129.15.64.216 On: Sun, 25 Sep 2016 17:34:16

TABLE II. Properties of the SWM6, TIP3P, and SWM4-NDP water models along with the corresponding experimental data. (Data for additional water models can be found in the supplementary material.[40])

	TIP3P[a]	SWM4-NDP[b]	SWM6[b,c]	Expt.[d]
Monomer				
μ_0 (D)	2.35	1.85	1.85	1.85
α (Å^3)		0.97825	0.88	1.44
Q_{xx} (DÅ)	−0.08	−0.248	−0.296	−0.13 (0.03)
Q_{yy} (DÅ)	1.76	2.425	2.385	2.63 (0.02)
Q_{zz} (DÅ)	−1.68	−2.177	−2.089	−2.50 (0.02)
Dimer				
U_{dimer} (kcal/mol)	−6.50	−5.15	−5.27	−5.44 (0.70)
d_{OO} (Å)	2.74	2.83	2.79	2.98 (0.01)
θ_A (°)	27	71	57	58 (6)
θ_D (°)	52	57	56	51 (6)
μ_{dimer} (D)	3.866	2.062	2.480	2.643
Air/water interface				
γ (dyn/cm)	52.7 (1.5)	65 (1)	60 (1)	71.99 (0.05)
$\Delta\phi$ (mV)	−500	−572 (18)	−558 (9)	
Liquid				
Δu (kcal/mol)	−9.82 (0.01)	−9.856 (0.010)	−9.931 (0.015)	−9.92
$\langle v \rangle$ (Å^3)	29.86 (0.03)	30.095 (0.047)	30.029 (0.048)	30.004
$\langle \mu \rangle$ (D)	2.35	2.459 (0.001)	2.431 (0.001)	2.95 (0.2)
ε	82 (5)	78.0 (1.4)	78.1 (2.8)	78.4 (0.1)
τ_D (ps)	5.1 (0.1)	9 (3)	10 (3)	8.24 (0.40)
D_{PBC} (10^{-5} cm^2/s)	5.123 (0.027)	2.35 (0.20)	1.76 (0.13)	
D_0 (10^{-5} cm^2/s)	6.14 (0.06)	2.85 (0.28)	2.14 (0.19)	2.3
η (cP)	0.308 (0.010)	0.66 (0.09)	0.87 (0.12)	0.89
τ_2^{HH} (ps)	0.8 (0.1)	1.8 (0.2)	2.4 (0.3)	2.1
ΔG_{hydr} (kcal/mol)	−6.10 (0.03)	−5.82 (0.08)	−5.74 (0.07)	−6.324
TMD (K)	182	< 220	235	277
ρ_{TMD} (g/cm^3)	1.038		1.019	1.000

[a] μ_{dimer} from Ref. 27, γ and $\Delta\phi$ from Ref. 100, D_{PBC} was calculated in Ref. 31 based on a cubic simulation cell with 256 water molecules, ε, τ_D and τ_2^{HH} from Ref. 101, D_0 and η are also taken from Ref. 31, ΔG_{hydr} from Ref. 102, TMD and ρ_{TMD} from Ref. 37, all other properties from Ref. 9. Uncertainties are given in parentheses if reported. The three components of the traceless quadrupole are defined using center of mass as origin, the origin-oxygen direction as X axis, the hydrogen-hydrogen direction as Y axis, and the perpendicular direction as Z axis.

[b] Instead of directly taken from the original paper, properties for SWM4-NDP were re-evaluated here using the same simulation setups as used for SWM6. Uncertainties are given in parentheses.

[c] The SWM6 20 × 150 ps MD simulations were repeated with a 12 Å cutoff for the L-J and real-space electrostatic interactions, yielding results within the error estimations of the presented results performed with at 15 Å cutoff. The calculated liquid properties using a box of 1000 waters run for 5 × 4 ns simulations are within the error estimations of the presented results (see Table S4 of the supplementary material[40]).

[d] μ_0 from Ref. 39, α from Ref. 74, quadrupoles from Ref. 103, dimer properties from Refs. 32 and 104, γ from Ref. 105, Δu from Ref. 106 using Eq. (4), $\langle v \rangle$ calculated from density data in Ref. 107, $\langle \mu \rangle$ cannot be directly measured from experiment and the value listed here was evaluated using mean-field approach from related experimental data in Ref. 108 and it should be noted that the calculated literature values range from 2.6 to 3.0 D.[26] ε from Ref. 109, τ_D from Ref. 110, D_0 from Ref. 53, η from Ref. 54, τ_2^{HH} from Ref. 111, ΔG_{hydr} from Ref. 112, and TMD and ρ_{TMD} from Ref. 113. Uncertainties are given in parentheses if available.

on the M site, the three components of the quadrupole moment can be reproduced to a quality similar to that of the SWM4-NDP model without using unphysical LP geometries as discussed above. Though it is possible to accurately reproduce the quadrupole moments with the available degrees of freedom in a six-site model, for example, a six-site model (3P+2L_{146}+M) with a charge of one electron on the LP sites was found to exactly reproduce the QM level quadrupoles,[46] however, it has not been shown that such models can yield reasonable bulk phase properties. As mentioned above, the gas phase polarizability of SWM6 is significantly smaller than the experimental value of 1.44 Å^3 (Ref. 74) and such reduced polarizability is essential to reproduce the dielectric constant of the liquid as widely found in the development of polarizable models for other polar molecules.[75–77] Although the polarizability is 10% smaller that that of the SWM4-NDP model, the average molecular dipole $\langle \mu \rangle$ in the bulk phase is almost the same as shown in Table II. A reduced polarizability may be required to accurately model the bulk phase because no shielding function is introduced to damp inter-molecular electrostatic interactions at short distances, as done in the AMOEBA model.

With the presence of negatively charged LPs in SWM6, the minimum interaction energy U_{dimer} is more negative and the oxygen-oxygen distance d_{OO} is shorter for the water dimer as compared to the SWM4-NDP model. The experimental dimer geometry[32] is better reproduced with SWM6 compared to SWM4-NDP, with a smaller hydrogen bond acceptor angle. With this geometry, the total dipole of the dimer for SWM6 is considerably larger than that of SWM4-NDP and closer to the experimental value. The open angle geometry of the SWM4-NDP water dimer is a compromise designed to reproduce the tetrahedral hydrogen-bonding pattern in bulk phase water. However, such a compromise is not needed for a six-site

Reuse of AIP Publishing content is subject to the terms: https://publishing.aip.org/authors/rights-and-permissions. Downloaded to IP: 129.15.64.216 On: Sun, 25 Sep 2016 17:34:16

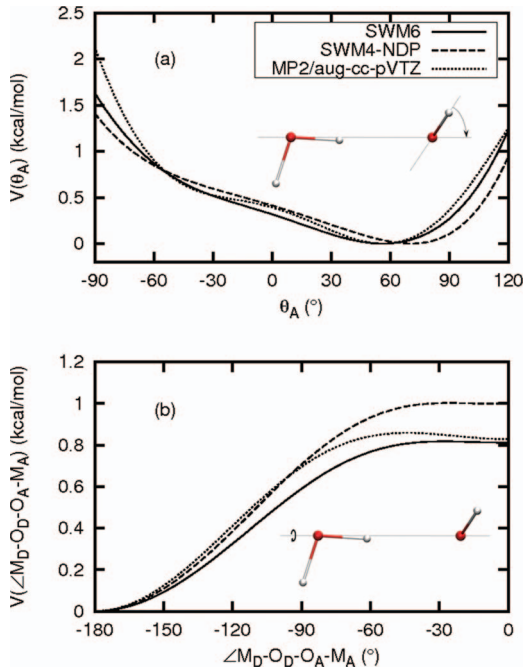

FIG. 3. Acceptor-angle (a) and rotational (b) PES scans of the water dimer. Flapping motion PES (a) is related to the angle θ_A defined by the acceptor water HOH bisector out of the axis through the two oxygen atoms and the rotational PES (b) is related to the rotation of the donor water around the axis through the two oxygen atoms, as shown by the inserted water dimer illustrations.

model as the presence of the LPs favors tetrahedral hydrogen bonding geometries. Alternatively, the flexible AMOEBA water model, which includes partial atomic charges, polarizabilities, dipole moments, and quadrupole moments on the oxygen and hydrogen sites, yields a water dimer O–O distance of 2.89 Å in better agreement with experiment while the acceptor and donor angles are similar to the present model.

Figure 3 shows dimer PES scans of the acceptor angle and rotation around the oxygen-oxygen axis. During the scans, the oxygen-oxygen distance was fixed to the equilibrium value from the corresponding QM or MM levels and the scan of the intermolecular degree of freedom was conducted with all other degrees of freedom fully optimized. Compared to the SWM4-NDP model, the SWM6 model better reproduced the global minimum position of the flapping PES (Figure 3(a)) and the barrier height of the rotational PES (Figure 3(b)) at the MP2/aug-cc-pVTZ level.

C. Water clusters

The performance of the SWM6 model on water clusters was investigated with respect to the high level calculations of Shields *et al.*[78] on systems of $(H_2O)_n$ with n = 3-10. The binding energies and the structural root mean-square deviations (RMSD) from QM geometries are presented in Table III. Instead of a global conformational search, full optimizations were directly conducted from the QM geometries using the MM models. Similar to the SWM4-NDP model, the SWM6 model estimates the binding energies to be less negative than the QM values, as also found for other polarizable models.[16,26] This is attributed to the scaled polarizability and it has been shown that more negative binding energies that are closer to the QM values can be obtained by using the experimental gas phase polarizability in a polarizable model.[26] However, with a smaller scaling factor, smaller deviations from the QM data are found for SWM6 with an average deviation of 2.45 kcal/mol compared to 3.32 kcal/mol for SWM4-NDP. This suggests that the more sophisticated charge distribution in SWM6 makes a larger contribution relative to the polarizability in reproducing the binding energies. Considering the relative stabilities for different isomers of a water cluster, both SWM4-NDP and SWM6 fail to recognize the most stable isomer for the water hexamer according to the QM data, though they capture the crosspoint feature that non-planer isomers become more stable than the cyclic ones beyond the water hexamer.[78] However, in contrast to the QM study, a recent rotational spectroscopy study suggested that the cage isomer is energetically more favorable than the prism isomer for the water hexamer[79] which is the case for the two polarizable models. So, if the experimental result is used as a reference, the four-site model gives the correct stability ordering for the hexamers, while six-site model fails to differentiate between the book and the cage isomers. As the energy differences between these hexamer isomers are quite small and no intramolecular geometry relaxation was allowed in the optimization of MM water clusters, the performance of the polarizable water models on water clusters with low hydrogen bonding coordination is quite acceptable. Both SWM4-NDP and SWM6 models can reproduce the QM hydrogen bonding structures reasonably well, with SWM6 performing slightly better as indicated by the smaller average structural RMSD. It should be noted that SWM4-NDP also fails to reproduce the relatively large energy difference of 1.57 kcal/mol between the PR1 and CA1 water heptamer isomers, while SWM6 model yields the correct stability ordering with an energy difference of 0.66 kcal/mol.

Interestingly, to the best of our knowledge, all site-based water models that can accurately reproduce the bulk phase properties overestimate (less negative) the cluster energies. On the other hand, a number of water models have been developed specifically targeting cluster energies during the optimization. For example, DPP2,[35] ASP-W4,[80] and TTM series of models[34,81] were developed for this purpose. However, these models, when used for bulk phase simulation, do not give satisfactory results. For example, the TTM3-F[34] and TTM2-R[81] all far overestimate the vaporization enthalpy of liquid water, though they can reproduce the QM water cluster energies accurately.

D. Air/water interface

To study if the SWM6 model can appropriately describe the anisotropic interfacial environment, the air/water interface properties were calculated. The surface tension γ was computed using Eq. (2) with the three diagonal pressure tensor components of the whole system[82] and the interfacial electrostatic potential was obtained by integrating the charge density $\rho(z)$ along the z axis that is perpendicular to the interface

Reuse of AIP Publishing content is subject to the terms: https://publishing.aip.org/authors/rights-and-permissions. Downloaded to IP: 129.15.64.216 On: Sun, 25 Sep 2016 17:34:16

TABLE III. Binding energies (kcal/mol) and structural root mean square deviations (RMSD, in Å) for water clusters $(H_2O)_{n=3-10}$.

		ab initio[a]	SWM4-NDP[b]			SWM6[b]		
n	Isomer	ΔE_{QM}	ΔE_{MM}	ΔE_{MM}-ΔE_{QM}	RMSD	ΔE_{MM}	ΔE_{MM}-ΔE_{QM}	RMSD
3	Cyclic	−14.92	−14.35	0.57	0.07	−14.38	0.54	0.08
4	Cyclic_S_4	−26.83	−25.10	1.73	0.07	−25.63	1.20	0.08
4	Cyclic_C_i	−25.86	−24.49	1.37	0.10	−25.06	0.80	0.10
5	Cyclic	−35.35	−33.25	2.10	0.18	−34.32	1.03	0.17
6	Prism	−45.31	−42.75	2.56	0.21	−43.01	2.30	0.47
6	Cage	−44.98	−43.05	1.93	0.17	−43.29	1.69	0.14
6	Book	−44.67	−42.45	2.22	0.22	−43.30	1.37	0.21
6	Cyclic	−43.62	−41.04	2.58	0.19	−42.52	1.10	0.20
7	PR1	−56.69	−53.83	2.86	0.21	−54.37	2.32	0.20
7	CA1	−55.12	−53.83	1.29	0.50	−53.71	1.41	0.28
7	CH1	−53.12	−50.77	2.35	0.59	−52.08	1.04	0.54
7	HM1	−51.14	−48.18	2.96	0.24	−49.67	1.47	0.26
8	D_{2d}	−72.27	−68.05	4.22	0.22	−68.73	3.54	0.22
8	S_4	−72.19	−67.75	4.44	0.14	−68.43	3.76	0.15
9	D_{2d}DDh	−81.46	−77.10	4.36	0.23	−78.37	3.09	0.23
9	S_4DAh-1	−81.16	−76.29	4.87	0.20	−77.42	3.74	0.20
9	S_4DDh-1	−81.00	−76.25	4.75	0.15	−77.41	3.59	0.16
9	D_{2d}DAh	−80.83	−76.02	4.81	0.31	−77.02	3.81	0.28
9	S_4DAnh-1	−80.76	−75.56	5.20	0.19	−76.55	4.21	0.18
10	PP1	−92.90	−88.24	4.66	0.22	−89.62	3.28	0.22
10	OB1	−91.24	−87.09	4.15	0.22	−88.02	3.22	0.22
10	DP1	−91.08	−85.30	5.78	0.19	−86.67	4.41	0.19
10	C1	−88.48	−83.79	4.69	0.45	−85.01	3.47	0.37
	Mean error			3.32	0.23		2.45	0.22

[a]MP2/CBS level results from Ref. 78.
[b]Optimized structure based on the QM structures. Structural RMSDs were calculated using only the three water atoms with QM coordinates as references.

using Eq. (3),

$$\gamma = \frac{L_z}{2}\left[\langle P_{zz}\rangle - \frac{(\langle P_{xx}\rangle + \langle P_{yy}\rangle)}{2}\right], \tag{2}$$

$$\phi(z) = -2\pi \int_{-\infty}^{z} dz' \left[\int_{-\infty}^{z'} dz''\rho(z'') - \int_{z'}^{\infty} dz''\rho(z'')\right]. \tag{3}$$

The γ value for the new model is somewhat smaller than that of SWM4-NDP model but is still closer to the experimental value as compared to TIP3P. With the explicit polarizability, the polarizable model can describe the anisotropic environment better than the additive model, which is optimized for an isotropic bulk environment and considers polarization in an average way. After plotting the electrostatic potential profile along the z axis (see Figure S3 in the supplementary material[40] for details), a fast potential drop is observed at the interface between −14 and −6 Å and a notable minimum at around −7.5 Å is found which corresponds to the average inward ordering of the molecular dipoles at the surface. After −6 Å, the potential becomes flat along with small fluctuations that correspond to the isotropic bulk phase behavior. The potential drop is estimated to be 558 mV, similar to the value of 572 mV for SWM4-NDP, and the total potential profile is quite similar to other polarizable models[83,84] but with a deeper well at the interface suggesting the enhanced description of the interfacial water structure by the SWM series of models. It has been shown that the value of the interfacial potential in polarizable models arise largely from the trace of the quadrupole moments.[85]

E. Bulk phase

The average net gain of internal energy upon liquefaction, Δu, which is related to the vaporization enthalpy, Δh, through Eq. (4) with subtraction of the thermal contribution from the Drude particle ($T_{Drude} = 1$ K) is well reproduced by the SWM6 model and the average molecular volume ⟨v⟩ is also close to the experimental value,

$$\Delta u = \langle u\rangle_{bulk} - \langle u\rangle_{gas} = \langle u\rangle_{bulk} - \frac{3}{2}k_B T_{Drude} = k_B T - \Delta h. \tag{4}$$

SWM6 yields a similar average molecular dipole ⟨μ⟩ as SWM4-NDP that falls into the range of 2.4-2.6 D, which has been suggested to be important to get the correct dielectric constant for simple water models.[26,86] The experimental value of 78.4 for the static dielectric constant is both perfectly reproduced by the SWM6 and SWM4-NDP model calculated using Eq. (5),[87] where M is the total dipole of the whole system and the high frequency dielectric constant ε_∞ is estimated from the Clausius-Mossotti equation.[88] As noticed before,[26,89] unlike other liquid properties, the evaluation of ε requires an extended simulation time for convergence (Figure S4 in the supplementary material[40]) and the convergence profiles obtained here are very similar to that presented for the SPC/E

Reuse of AIP Publishing content is subject to the terms: https://publishing.aip.org/authors/rights-and-permissions. Downloaded to IP: 129.15.64.216 On: Sun, 25 Sep 2016 17:34:16

model as studied by Gereben and Pusztai,[89]

$$\varepsilon = \varepsilon_\infty + \frac{4\pi}{3k_B T \langle V \rangle}(\langle M^2 \rangle - \langle M \rangle^2). \quad (5)$$

The dielectric relaxation was investigated as the Debye relaxation time τ_D evaluated from exponential fits of the decay of the total dipole autocorrelation function as defined in Eq. (6).[90] Similar to SWM4-NDP, the SWM6 model yields a larger relaxation time than the experimental value while the additive TIP3P give a faster dielectric relaxation,

$$C_M(t) = \frac{\langle M(t)M(0) \rangle}{\langle M^2 \rangle}. \quad (6)$$

The shear viscosity η was calculated from the integration of the time autocorrelation function of off-diagonal pressure tensor components with the Green-Kubo relation[91,92] using Eq. (7),

$$\eta = \frac{1}{3} \sum_{\alpha\beta=xy,yz,xz} \frac{V}{k_B T} \int_0^\infty dt \langle P_{\alpha\beta}(t) P_{\alpha\beta}(0) \rangle. \quad (7)$$

Similar to previously reported results,[93] the pressure autocorrelation function shows a fast decay and oscillations within 0.2 ps, followed by a slower decay (Figure S5(a) in the supplementary material[40]). Integrating the autocorrelation function gives the viscosity and its convergence can be found in Figure S5(b) in the supplementary material.[40] The evaluated η value of 0.87 cP for SWM6 is much closer to the experimental value of 0.89 cP than that of either SWM4-NDP or TIP3P.

The self-diffusion coefficient without system size correction, D_{PBC}, was calculated from the mean squared displacement of the center-of-mass (COM) of all molecules under the Stokes-Einstein relation[94] according to the Eq. (8). D_0 was computed using Eq. (9) as suggest by Yeh and Hummer[31] with the system size correction estimated using the calculated viscosity η. By targeting a value with size correction taken into account, the SWM6 model yields a D_0 value that is closer to the experimental data while the SWM4 model overestimates the self-diffusion coefficient but has a value that is significantly lower than that of the additive TIP3P model,

$$D_{PBC} = \lim_{t\to\infty} \frac{1}{6t} \left\langle \frac{1}{N} \sum_{i=1}^{N} [r_{COM,i}(t) - r_{COM,i}(0)]^2 \right\rangle, \quad (8)$$

$$D_0 = D_{PBC} + \frac{2.837297 k_B T}{6\pi\eta L}. \quad (9)$$

It should be noted that the system size correction had not been considered previously during development of most water models, which limits comparisons with experimental diffusion coefficient. For example, the diffusion coefficient for TIP4P-Ew water model was calculated to be 2.4×10^{-5} cm^2/s for a box of 512 water molecules in the original paper,[12] which is quite close to the experimental value. However, using the evaluated viscosity of 0.74 cP,[95] D_0 is calculated as $\sim 2.7 \times 10^{-5}$ cm^2/s using Eq. (9), which is larger than the experimental value. For some water models, the agreement between the calculated and experimental self-diffusion coefficient becomes even better when the system size correction is considered. For example, D_{PBC} was calculated to be 1.96 $\times 10^{-5}$ cm^2/s for a box of 512 water molecules[96] and η was calculated as 1.35 cP for the AMOEBA model,[15] which results in a D_0 value of 2.14×10^{-5} cm^2/s, much closer to the experimental value. According to our knowledge, besides the current work, the size correction was only considered in one water model development work published recently.[36] This suggests that reoptimization may be considered for those water models whose target data included the self-diffusion coefficient.

Rotational dynamics of the new model was investigated by calculating the NMR relaxation time τ_2^{HH}, which was evaluated from exponential fits of the long time decay of the correlation function[17] defined in Eq. (10) where the $\hat{u}_{HH}$ is the unit vector along the two hydrogen atoms within a water molecule,

$$C_{rot}(t) = \left\langle \frac{3}{2}[\hat{u}_{HH}(t) \cdot \hat{u}_{HH}(0)]^2 - \frac{1}{2} \right\rangle. \quad (10)$$

The obtained τ_2^{HH} value for SWM6 is somewhat larger than the experimental value while SWM4-NDP has an underestimated value. The additive TIP3P model significantly underestimates the experimental value by about 60%. The ordering of the relaxation time given by different models is consistent with the ordering of their diffusion coefficients. With a lower self-diffusion coefficient, a longer relaxation time is expected.

The hydration free energy was also calculated and listed in Table II. The resulting ΔG_{hydr} value of SWM6 model is quite similar to that of the SWM4-NDP model and satisfactorily reproduces the experiment value when considering the wide uncertainty range of the experimental data.[27]

Atom-atom radial distribution functions (RDF) of the SWM6 model are presented in Figure 4 along with those of SWM4-NDP and experimental data.[97] Considering the

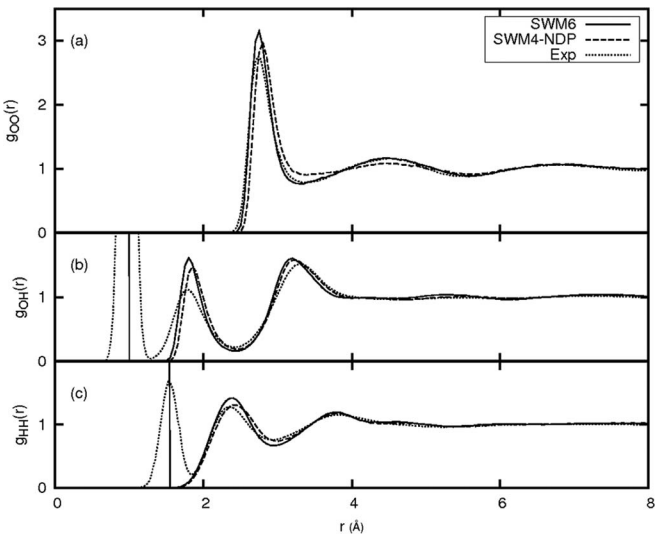

FIG. 4. Radial distribution functions of the oxygen-oxygen (a), oxygen-hydrogen (b), and hydrogen-hydrogen (c) atom pairs. Experimental neutron diffraction data is from Ref. 97.

Reuse of AIP Publishing content is subject to the terms: https://publishing.aip.org/authors/rights-and-permissions. Downloaded to IP: 129.15.64.216 On: Sun, 25 Sep 2016 17:34:16

TABLE IV. NMR shielding σ^H and chemical shift $\Delta\sigma^H$ (relative to the gas phase) of the water hydrogen atoms calculated for the SWM6, SWM4-NDP, TIP5P-Ew, TIP4P/2005, TIP4P-Ew, and TIP3P water models.

	σ^H		$\Delta\sigma^H$ [a]	
	Cal.	Cal.-Expt.[b]	Cal.	Cal.-Expt.[b]
SWM6	25.71	−0.08	−3.92	0.34
SWM4-NDP	26.14	0.35	−3.49	0.77
TIP5P-Ew[c]	26.03	0.24	−3.60	0.66
TIP4P/2005[c]	26.31	0.52	−3.32	0.94
TIP4P-Ew[c]	25.90	0.11	−3.73	0.53
TIP3P[d]	26.37	0.58	−3.26	1.00

[a]Gaseous water hydrogen NMR shielding is evaluated to be 29.63 ppm using the current calculation method for all models as they adopt the same water geometry, and compared to the experimental value of 30.05 ppm.[98]
[b]Experimental value for shielding and chemical shift is 25.79 and −4.26 ppm, respectively.[98]
[c]The parameter files for these water models in CHARMM format are available from the CHARMM parameter download page (http://mackerell.umaryland.edu/CHARMM_ff_params.html).
[d]CHARMM version of the original TIP3P model.

oxygen-oxygen RDF, though the height of the first peak in the $g_{OO}(r)$ is more overestimated by the SWM6 model, the position of the first peak is better reproduced compared to the outward shift by the SWM4-NDP model. The shape of the first minimum and the second peak in the $g_{OO}(r)$ are also better reproduced by the new model, while the SWM4-NDP model has a higher first minimum and lower second peak. This indicates that the new model has a more ordered water shell structure than the SWM4-NDP model. Compared to several other water models (Table S1 in the supplementary material[40]), the new model also shows better agreement with the experimental oxygen-oxygen RDF, especially for the positions and heights of the first minimum and the second peak. For example, deviations of positions and heights of the first trough and the second peak for AMOEBA water model are 0.19 Å, 0.10, 0.15 Å, and −0.05, respectively, while the respective values are −0.01 Å, −0.02, −0.05 Å, and 0.01 for the new SWM6 model. For the oxygen-hydrogen and hydrogen-hydrogen RDFs, similar plots are obtained for the new and the four-site models, which agree with the experimental data, with the SWM6 model showing a slight improvement in the location of the first maximum for both RDFs.

The good performance of SWM6 in reproducing the experimental $g_{OO}(r)$ suggests that the local water structure in bulk phase is better reproduced with the new model. To further characterize properties related to the local water structure, NMR shielding, and the related chemical shifts, which are sensitive indictors of the local hydrogen bonding structure, were calculated following the protocol used by Banyai *et al.*[68] It was shown that the applied density functional method based protocol can give chemical shifts that are close to the experimental value for the bulk water structures collected from *ab initio* MD simulations.[68] The results are shown in Table IV and the SWM6 model yields the best agreement with the experimental data[98] (25.71 vs 25.79 ppm for σ^H and −3.92 vs −4.26 ppm for $\Delta\sigma^H$) followed by TIP4P-Ew, TIP5P-Ew, SWM4-NDP, and TIP4P/2005, while the CHARMM version of the TIP3P model gives the highest deviations. The calculated NMR properties seem to be very dependent on the calculation protocols, for example, shielding σ^H and chemical shift $\Delta\sigma^H$ were calculated to be 28.36 and −2.53 ppm for the TIP3P model by Kongsted *et al.* using a QM/MM method.[99] However, with the same simulation setups as used by Banyai *et al.*,[68] it can be concluded that the SWM6 model yields local hydrogen bonding structures that are closer to the *ab initio* MD structures when compared to the other tested models.

Since the new water model is developed as a more accurate version of the SWM water models, the above discussions mainly concentrated on comparisons with SWM4-NDP and the commonly used additive TIP3P model. However, performance of the SWM6 model is also quite competitive when compared to other water models as shown in Tables S2 and S3 in the supplementary material.[40] For those models for which the appropriate data is available, the accumulated absolute percentage differences of important monomer, dimer, and liquid properties are summarized in Table V and compared to the new model. The overall percentage differences are consistent with the general consensus. That is, the performance improves with an increased site number in the TIP series of water models (i.e., TIP3P, TIP4P, and TIP5P). The advanced versions of the TIP4P model, TIP4P-Ew, and TIP4P/2005, have better performances than the TIP4P and the polarizable models perform better than additive models. The new SWM6 model shows significant improvement over all the additive models as well as the more sophisticated AMOEBA polarizable model.

Though not optimized for simulations under non-ambient temperature and pressure conditions, the temperature dependence of liquid density was investigated in order to understand the performance of SWM4-NDP and SWM6 water models

TABLE V. Accumulated absolute percentage differences (%) between calculated and experimental monomer, dimer, and liquid properties for several water models.[a]

	TIP3P	TIP4P	TIP4P-Ew	TIP4P/2005	TIP5P	SPC/E	AMOEBA	SWM4-NDP	SWM6
Monomer[b]	60	34	41	35	61	44	9	8	9
Dimer[c]	127	46	82	58	57	144	17	55	17
Liquid[d]	259	165	77	61	82	73	69	68	27
Overall	446	245	201	154	200	261	95	130	54

[a]See Tables S2 and S3 of the supplementary material[40] for the values of the included properties for the respective models.
[b]Monomer properties include μ_0 and Q_{yy}.
[c]Dimer properties include U_{dimer}, d_{OO}, θ_A, and μ_{dimer}.
[d]Liquid properties under ambient conditions include Δu, $\langle v\rangle$, $\langle\mu\rangle$, ε, D_0, and η.

Reuse of AIP Publishing content is subject to the terms: https://publishing.aip.org/authors/rights-and-permissions. Downloaded to IP: 129.15.64.216 On: Sun, 25 Sep 2016 17:34:16

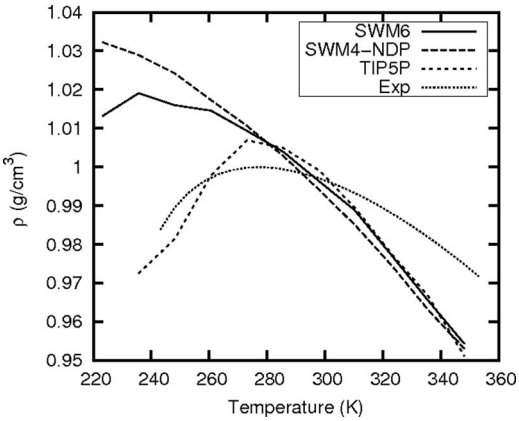

FIG. 5. Temperature dependence of the liquid density of water at 1 atm. Experimental data from Ref. 107 and TIP5P data from Ref. 9.

over a wide temperature range (Figure 5). Results for the additive TIP5P model, which was optimized to capture the density anomaly of water, are also shown in the figure. Generally speaking, compared to the experimental data, the densities of all models decrease too fast with increasing temperature above 300 K, with the densities of the SWM6 model slightly closer to the experimental data as compared to the SWM4-NDP model. The SWM6 model shows a density maximum around 235 K, which underestimates the experimental temperature of maximum density (TMD) by about 40 K; the SWM4-NDP model does not show a density maximum above 220 K. The TIP5P model reproduces the correct TMD.

Since the liquid densities at various temperatures or the TMD was not included as target data during the optimization, as done for the TIP5P,[9] TIP4P-Ew,[12] and TIP4P/2005[13] water models, it is not surprising that the new model does not reproduce the experimental temperature dependence of the density. But it is still promising to see a peak, which is an improvement over the SWM4-NDP model, though the TMD is underestimated by 40 K. Recently, Kiss and Baranyai discussed why the site-based rigid polarizable models typically do not get the correct temperature dependence of density compared to additive models.[37] It was suggested that the polarization decreases with increasing temperature due to a loss of hydrogen bonding, a phenomenon that cannot occur in additive models, leading to a larger decrease in the density of water at higher temperatures. This phenomenon also leads to an enhanced increase in the density at lower temperatures. Flexible polarizable models, such as AMOEBA,[15] partially overcome the problem by allowing internal geometry changes, which were found to make an important contribution to the anomalous density maximum.[96]

To the best of our knowledge, no site-based model, including both additive and polarizable models, can reproduce both the TMD and properties under ambient conditions to a high accuracy. For example, TIP4P-Ew[12] and TIP4P/2005[13] have the correct TMD, but the dielectric constant at 298 K is underestimated by 18% and 23%, respectively, and the self-diffusion coefficient is overestimated by 19% and 8%, respectively. TIP5P[9] and TIP5P-Ew[14] have the correct TMD and their dielectric constants are much closer to the experimental value, but the self-diffusion coefficients are even more overestimated compared to the four-site models. The polarizable AMOEBA model has a reasonable TMD[96] and satisfactorily reproduces both the dielectric constant and self-diffusion constant; however, it overestimates the viscosity by 52%. While not the final word, this analysis indicates that site-based models can either reproduce the TMD or the properties under ambient conditions to a high level of accuracy. In the current model, we focused on the properties under ambient conditions, which are more relevant for that majority of MD simulations of biological systems.

IV. CONCLUSION

A new six-site polarizable model of water, SWM6, for which LP sites were introduced into the SWM4-NDP model followed by additional optimization, is presented. The new model has a similar M site geometry as its four-site predecessor. The distance between the LP sites and the oxygen atom is 0.315 Å, which is similar to the distance obtained from QM electrostatic analyses[46] suggesting the physical relevance of the LP positions in the SWM6 model. The overall quality of the new model on bulk phase water is comparable to the SWM4 models while the self-diffusion coefficient was corrected for the system size effect in the new model. With a more sophisticated charge distribution, the dimer properties are better reproduced as are the relative energies of water clusters. Overall, the new model has an improved balance between descriptions of microscopic and bulk phase properties, compared to most additive and polarizable water models developed previously. Moreover, the local hydrogen bonding structures in the liquid phase are better reproduced in the new model as indicated by the $g_{OO}(r)$ and NMR properties. However, the temperature dependence of the SWM6 water model, though better than the SWM4-NDP model, still does not correctly model the density maximum in agreement with experiment.

It should be noted that the newly developed SWM6 model has not been tested with respect to solvation properties of ions and other types of molecules. Preliminary data indicates that the hydration free energy of one SWM6 water in a box of SWM4-NDP waters is similar to that of one SWM4-NDP water in a box of SWM6 waters and also similar to that for pure SWM4-NDP or SWM6 bulk water (not shown). While this is not sufficient to say that the new water model is fully compatible with the CHARMM Drude force field, it indicates the compatibility of the models and more tests of the model with respect to this important property will be undertaken. It should also be noted that the new model is not developed for routine use but rather to be considered when the local hydrogen bonding of water is important and high accuracy is needed. The computational demand of SWM6 is estimated to be approximately two times more than that of SWM4-NDP and five times more that that of TIP3P based on simulations of 216 water molecules on an 8 core node with version 36 of CHARMM. The newly developed SWM6 model will be available as part of the CHARMM polarizable force field topology and parameter files on the website of the MacKerell laboratory (http://mackerell.umaryland.edu/).

Reuse of AIP Publishing content is subject to the terms: https://publishing.aip.org/authors/rights-and-permissions. Downloaded to IP: 129.15.64.216 On: Sun, 25 Sep 2016 17:34:16

ACKNOWLEDGMENTS

This work is supported by National Institutes of Health (NIH) (Grant Nos. GM051501, GM072558, and GM070855). Supercomputer time provided by the Teragrid computational resources is acknowledged. The authors are grateful to Dr. Guillaume Lamoureux and Dr. Edward Harder for their assistance and for helpful discussions.

[1] *Computational Biochemistry and Biophysics*, edited by O. M. Becker, A. D. MacKerell, Jr., B. Roux, and M. Watanabe (Marcel Dekker, New York, 2001).
[2] G. W. Robinson, S. Zhu, S. Singh, and M. W. Evans, *Water in Biology, Chemistry and Physics: Experimental Overviews and Computational Methodologies* (World Scientific, Singapore, 1996).
[3] B. Guillot, J. Mol. Liq. **101**, 219 (2002).
[4] W. L. Jorgensen and J. Tirado-Rives, Proc. Natl. Acad. Sci. U.S.A. **102**, 6665 (2005).
[5] C. Vega, J. L. F. Abascal, M. M. Conde, and J. L. Aragones, Faraday Discuss. **141**, 251 (2009).
[6] H. J. C. Berendsen, J. P. M. Postma, W. F. v. Gunsteren, and J. Hermans, in *Intermolecular Forces*, edited by B. Pullman (Reidel, Dordrecht, 1981), p. 331.
[7] W. L. Jorgensen, J. Am. Chem. Soc. **103**, 335 (1981).
[8] W. L. Jorgensen, J. Chandrasekhar, J. D. Madura, R. W. Impey, and M. L. Klein, J. Chem. Phys. **79**, 926 (1983).
[9] M. W. Mahoney and W. L. Jorgensen, J. Chem. Phys. **112**, 8910 (2000).
[10] H. J. C. Berendsen, J. R. Grigera, and T. P. Straatsma, J. Phys. Chem. **91**, 6269 (1987).
[11] F. H. Stillinger and A. Rahman, J. Chem. Phys. **60**, 1545 (1974).
[12] H. W. Horn, W. C. Swope, J. W. Pitera, J. D. Madura, T. J. Dick, G. L. Hura, and T. Head-Gordon, J. Chem. Phys. **120**, 9665 (2004).
[13] J. L. F. Abascal and C. Vega, J. Chem. Phys. **123**, 234505 (2005).
[14] S. W. Rick, J. Chem. Phys. **120**, 6085 (2004).
[15] P. Ren and J. W. Ponder, J. Phys. Chem. B **107**, 5933 (2003).
[16] H. Yu and W. F. van Gunsteren, J. Chem. Phys. **121**, 9549 (2004).
[17] S. W. Rick, S. J. Stuart, and B. J. Berne, J. Chem. Phys. **101**, 6141 (1994).
[18] I. M. Svishchev, P. G. Kusalik, J. Wang, and R. J. Boyd, J. Chem. Phys. **105**, 4742 (1996).
[19] L. X. Dang and T. M. Chang, J. Chem. Phys. **106**, 8149 (1997).
[20] H. Saint-Martin, J. Hernandez-Cobos, M. I. Bernal-Uruchurtu, I. Ortega-Blake, and H. J. C. Berendsen, J. Chem. Phys. **113**, 10899 (2000).
[21] H. A. Stern, F. Rittner, B. J. Berne, and R. A. Friesner, J. Chem. Phys. **115**, 2237 (2001).
[22] P. J. van Maaren and D. van der Spoel, J. Phys. Chem. B **105**, 2618 (2001).
[23] P. Drude, Ann. Phys. **306**, 566 (1900).
[24] P. Drude, Ann. Phys. **308**, 369 (1900).
[25] G. Lamoureux and B. Roux, J. Chem. Phys. **119**, 3025 (2003).
[26] G. Lamoureux, A. D. MacKerell, and B. Roux, J. Chem. Phys. **119**, 5185 (2003).
[27] G. Lamoureux, E. Harder, I. V. Vorobyov, B. Roux, and A. D. MacKerell, Chem. Phys. Lett. **418**, 245 (2006).
[28] G. Archontis, E. Leontidis, and G. Andreou, J. Phys. Chem. B **109**, 17957 (2005).
[29] H. Yu, C. L. Mazzanti, T. W. Whitfield, R. E. Koeppe, O. S. Andersen, and B. Roux, J. Am. Chem. Soc. **132**, 10847 (2010).
[30] W. Jiang, D. J. Hardy, J. C. Phillips, A. D. MacKerell, K. Schulten, and B. Roux, J. Phys. Chem. Lett. **2**, 87 (2011).
[31] I. C. Yeh and G. Hummer, J. Phys. Chem. B **108**, 15873 (2004).
[32] T. R. Dyke, K. M. Mack, and J. S. Muenter, J. Chem. Phys. **66**, 498 (1977).
[33] E. Harder, V. M. Anisimov, I. V. Vorobyov, P. E. M. Lopes, S. Y. Noskov, A. D. MacKerell, and B. Roux, J. Chem. Theory Comput. **2**, 1587 (2006).
[34] G. S. Fanourgakis and S. S. Xantheas, J. Chem. Phys. **128**, 074506 (2008).
[35] R. Kumar, F. Wang, G. R. Jenness, and K. D. Jordan, J. Chem. Phys. **132**, 014309 (2010).
[36] L. Viererblova and J. Kolafa, Phys. Chem. Chem. Phys. **13**, 19925 (2011).
[37] P. T. Kiss and A. Baranyai, J. Chem. Phys. **137**, 084506 (2012).
[38] J. L. Aragones, L. G. MacDowell, and C. Vega, J. Phys. Chem. A **115**, 5745 (2011).
[39] T. R. Dyke and J. S. Muenter, J. Chem. Phys. **59**, 3125 (1973).
[40] See supplementary material http://dx.doi.org/10.1063/1.4774577 for Figures S1-S5, Tables S1-S4, and the SA setup.
[41] J. L. F. Abascal and C. Vega, J. Phys. Chem. C **111**, 15811 (2007).
[42] T. Ichiye and M. Tan, J. Chem. Phys. **124**, 134504 (2006).
[43] G. A. Tribello and B. Slater, Chem. Phys. Lett. **425**, 246 (2006).
[44] C. Vega and P. A. Monson, J. Chem. Phys. **102**, 1361 (1995).
[45] S. L. Carnie and G. N. Patey, Mol. Phys. **47**, 1129 (1982).
[46] S. Niu, M. Tan, and T. Ichiye, J. Chem. Phys. **134**, 134501 (2011).
[47] W. S. Benedict, N. Gailar, and E. K. Plyler, J. Chem. Phys. **24**, 1139 (1956).
[48] B. R. Brooks, C. L. Brooks III, A. D. Mackerell, Jr., L. Nilsson, R. J. Petrella, B. Roux, Y. Won, G. Archontis, C. Bartels, S. Boresch, A. Caflisch, L. Caves, Q. Cui, A. R. Dinner, M. Feig, S. Fischer, J. Gao, M. Hodoscek, W. Im, K. Kuczera, T. Lazaridis, J. Ma, V. Ovchinnikov, E. Paci, R. W. Pastor, C. B. Post, J. Z. Pu, M. Schaefer, B. Tidor, R. M. Venable, H. L. Woodcock, X. Wu, W. Yang, D. M. York, and M. Karplus, J. Comput. Chem. **30**, 1545 (2009).
[49] H. Nada and J. P. J. M. van der Eerden, J. Chem. Phys. **118**, 7401 (2003).
[50] S. Kirkpatrick, C. D. Gelatt, and M. P. Vecchi, Science **220**, 671 (1983).
[51] A. Corana, M. Marchesi, C. Martini, and S. Ridella, ACM Trans. Math. Softw. **13**, 262 (1987).
[52] W. L. Goffe, G. D. Ferrier, and J. Rogers, J. Econometr. **60**, 65 (1994).
[53] K. Krynicki, C. D. Green, and D. W. Sawyer, Faraday Discuss. Chem. Soc. **66**, 199 (1978).
[54] K. R. Harris and L. A. Woolf, J. Chem. Eng. Data **49**, 1064 (2004).
[55] R: A Language and Environment for Statistical Computing (R Foundation for Statistical Computing, Vienna, Austria, 2011).
[56] T. Darden, D. York, and L. Pedersen, J. Chem. Phys. **98**, 10089 (1993).
[57] M. P. Allen and D. J. Tildesley, *Computer Simulation of Liquids* (Oxford University Press, Oxford, England, 1987).
[58] G. J. Martyna, M. E. Tuckerman, D. J. Tobias, and M. L. Klein, Mol. Phys. **87**, 1117 (1996).
[59] W. G. Hoover, Phys. Rev. A **31**, 1695 (1985).
[60] S. Nosé, Mol. Phys. **52**, 255 (1984).
[61] C. Møller and M. S. Plesset, Phys. Rev. **46**, 618 (1934).
[62] J. T. H. Dunning, J. Chem. Phys. **90**, 1007 (1989).
[63] M. J. Frisch, G. W. Trucks, H. B. Schlegel *et al.*, GAUSSIAN 03, Revision C.02, Gaussian Inc., Wallingford, CT, 2003.
[64] Y. Deng and B. Roux, J. Phys. Chem. B **108**, 16567 (2004).
[65] S. Kumar, J. M. Rosenberg, D. Bouzida, R. H. Swendsen, and P. A. Kollman, J. Comput. Chem. **13**, 1011 (1992).
[66] D. Sebastiani and M. Parrinello, J. Phys. Chem. A **105**, 1951 (2001).
[67] D. Sebastiani and M. Parrinello, ChemPhysChem **3**, 675 (2002).
[68] D. R. Banyai, T. Murakhtina, and D. Sebastiani, Magn. Reson. Chem. **48**, S56 (2010).
[69] A. D. Becke, Phys. Rev. A **38**, 3098 (1988).
[70] C. Lee, W. Yang, and R. G. Parr, Phys. Rev. B **37**, 785 (1988).
[71] S. Goedecker, M. Teter, and J. Hutter, Phys. Rev. B **54**, 1703 (1996).
[72] CPMD, version 3.15, Copyright IBM Corp. 1990-2008 and Copyright MPI für Festkörperforschung Stuttgart 1997-2001, http://www.cpmd.org.
[73] S. R. Durell, B. R. Brooks, and A. Ben-Naim, J. Phys. Chem. **98**, 2198 (1994).
[74] F. H. Stillinger, in *The Liquid State of Matter: Fluids Simple and Complex*, edited by E. W. Montroll and J. L. Lebowitz (North-Holland, Amsterdam, 1982).
[75] X. Zhu, P. E. M. Lopes, and A. D. MacKerell, WIREs: Comput. Mol. Sci. **2**, 167 (2012).
[76] I. V. Vorobyov, V. M. Anisimov, and A. D. MacKerell, J. Phys. Chem. B **109**, 18988 (2005).
[77] P. E. M. Lopes, G. Lamoureux, B. Roux, and A. D. MacKerell, J. Phys. Chem. B **111**, 2873 (2007).
[78] R. M. Shields, B. Temelso, K. A. Archer, T. E. Morrell, and G. C. Shields, J. Phys. Chem. A **114**, 11725 (2010).
[79] C. Perez, M. T. Muckle, D. P. Zaleski, N. A. Seifert, B. Temelso, G. C. Shields, Z. Kisiel, and B. H. Pate, Science **336**, 897 (2012).
[80] M. P. Hodges, A. J. Stone, and S. S. Xantheas, J. Phys. Chem. A **101**, 9163 (1997).
[81] C. J. Burnham and S. S. Xantheas, J. Chem. Phys. **116**, 1500 (2002).
[82] J. G. Kirkwood and F. P. Buff, J. Chem. Phys. **17**, 338 (1949).
[83] C. D. Wick, I. F. W. Kuo, C. J. Mundy, and L. X. Dang, J. Chem. Theory Comput. **3**, 2002 (2007).
[84] V. P. Sokhan and D. J. Tildesley, Mol. Phys. **92**, 625 (1997).
[85] E. Harder and B. Roux, J. Chem. Phys. **129**, 234706 (2008).
[86] M. Sprik, J. Chem. Phys. **95**, 6762 (1991).
[87] M. Neumann and O. Steinhauser, Chem. Phys. Lett. **106**, 563 (1984).
[88] P. V. Rysselberghe, J. Phys. Chem. **36**, 1152 (1931).

Reuse of AIP Publishing content is subject to the terms: https://publishing.aip.org/authors/rights-and-permissions. Downloaded to IP: 129.15.64.216 On: Sun, 25 Sep 2016 17:34:16

[89]O. Gereben and L. Pusztai, Chem. Phys. Lett. **507**, 80 (2011).
[90]M. Neumann and O. Steinhauser, Chem. Phys. Lett. **102**, 508 (1983).
[91]M. S. Green, J. Chem. Phys. **22**, 398 (1954).
[92]R. Kubo, J. Phys. Soc. Jpn. **12**, 570 (1957).
[93]S. Tazi, A. Botan, M. Salanne, V. Marry, P. Turq, and B. Rotenberg, J. Phys.: Condens. Matter **24**, 284117 (2012).
[94]A. Einstein, Ann. Phys. **322**, 549 (1905).
[95]A. P. Markesteijn, R. Hartkamp, S. Luding, and J. Westerweel, J. Chem. Phys. **136**, 134104 (2012).
[96]P. Ren and J. W. Ponder, J. Phys. Chem. B **108**, 13427 (2004).
[97]A. K. Soper, Chem. Phys. **258**, 121 (2000).
[98]J. C. Hindman, J. Chem. Phys. **44**, 4582 (1966).
[99]J. Kongsted, C. B. Nielsen, K. V. Mikkelsen, O. Christiansen, and K. Ruud, J. Chem. Phys. **126**, 034510 (2007).
[100]S. E. Feller, R. W. Pastor, A. Rojnuckarin, S. Bogusz, and B. R. Brooks, J. Phys. Chem. **100**, 17011 (1996).
[101]D. van der Spoel, P. J. van Maaren, and H. J. C. Berendsen, J. Chem. Phys. **108**, 10220 (1998).
[102]M. R. Shirts and V. S. Pande, J. Chem. Phys. **122**, 134508 (2005).
[103]J. Verhoeven and A. Dymanus, J. Chem. Phys. **52**, 3222 (1970).
[104]L. A. Curtiss, D. J. Frurip, and M. Blander, J. Chem. Phys. **71**, 2703 (1979).
[105]N. R. Pallas and Y. Harrison, Colloids Surf. **43**, 169 (1990).
[106]*Recommended Reference Materials for the Realization of Physicochemical Properties*, edited by K. N. Marsh (Blackwell, Oxford, 1987).
[107]G. S. Kell, J. Chem. Eng. Data **20**, 97 (1975).
[108]A. V. Gubskaya and P. G. Kusalik, J. Chem. Phys. **117**, 5290 (2002).
[109]D. P. Fernandez, Y. Mulev, A. R. H. Goodwin, and J. M. H. L. Sengers, J. Phys. Chem. Ref. Data **24**, 33 (1995).
[110]J. T. Kindt and C. A. Schmuttenmaer, J. Phys. Chem. **100**, 10373 (1996).
[111]J. Jonas, T. DeFries, and D. J. Wilbur, J. Chem. Phys. **65**, 582 (1976).
[112]A. Ben-Naim and Y. Marcus, J. Chem. Phys. **81**, 2016 (1984).
[113]D. E. Hare and C. M. Sorensen, J. Chem. Phys. **84**, 5085 (1986).

Reuse of AIP Publishing content is subject to the terms: https://publishing.aip.org/authors/rights-and-permissions. Downloaded to IP: 129.15.64.216 On: Sun, 25 Sep 2016 17:34:16